

A Low-Cost Vision-Based Tactile Gripper with Pretraining Learning for Contact-Rich Manipulation

Yaohua Liu, Binkai Ou*, Zicheng Qiu, Ce Hao, Yemin Wang and Hengjun Zhang*

Abstract— Robotic manipulation in contact-rich environments remains challenging, particularly when relying on conventional tactile sensors that suffer from limited sensing range, reliability, and cost-effectiveness. In this work, we present LVTG, a low-cost visuo-tactile gripper designed for stable, robust, and efficient physical interaction. Unlike existing visuo-tactile sensors, LVTG enables more effective and stable grasping of larger and heavier everyday objects, thanks to its enhanced tactile sensing area and greater opening angle. Its surface skin is made of highly wear-resistant material, significantly improving durability and extending operational lifespan. The integration of vision and tactile feedback allows LVTG to provide rich, high-fidelity sensory data, facilitating reliable perception during complex manipulation tasks. Furthermore, LVTG features a modular design that supports rapid maintenance and replacement. To effectively fuse vision and touch, We adopt a CLIP-inspired contrastive learning objective to align tactile embeddings with their corresponding visual observations, enabling a shared cross-modal representation space for visuo-tactile perception. This alignment improves the performance of an Action Chunking Transformer (ACT) policy in contact-rich manipulation, leading to more efficient data collection and more effective policy learning. Compared to the original ACT method, the proposed LVTG with pretraining achieves significantly higher success rates in manipulation tasks.

Index Terms— Vision-Based Tactile Sensor, Manipulation, Robot Learning, Action Chunking Transformer

arXiv:2602.00514v1 [cs.RO] 31 Jan 2026

I. INTRODUCTION

HUMANS possess a remarkable capacity to perform complex manipulation tasks that involve rich physical contact, such as handling fragile or deformable objects, by effectively fusing visuo and tactile information. Vision plays a key role in object recognition and spatial localization, while tactile sensing provides real-time feedback on local contact conditions, including surface texture, material compliance, and force distribution, which are typically inaccessible through vision alone [1]–[3]. For instance, when interacting with delicate items, visuo cues guide the initial reaching and grasping motions, and tactile signals enable continuous, fine-grained adjustments to grip strength and orientation to prevent damage.

Manuscript received xx, xx, xx. (Corresponding author: Binkai Ou and Hengjun Zhang.)

Yaohua Liu is with the Guangdong Institute of Intelligence Science and Technology, Hengqin, Zhuhai, 519031, Guangdong, China.

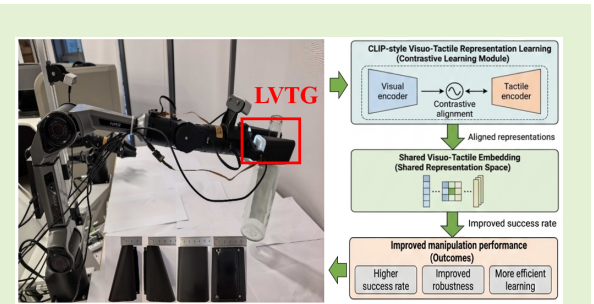
Binkai Ou is with the Innovation and Research and Development Department, BoardWare Information System Company Ltd., Macau 999078, China.

Zicheng Qiu is with the School of Artificial Intelligence, Nanjing Agricultural University, Nanjing 210095, China and the Guangdong Institute of Intelligence Science and Technology, Hengqin, Zhuhai, 519031, Guangdong, China.

Ce Hao is with the School of Computing, National University of Singapore.

Yemin Wang is with the School of Aerospace Engineering, Xiamen University, Xiamen 361005, China.

Hengjun Zhang is with the School of Electronic Engineering and Automation, Guilin University of Electronic Technology, Guilin 541000, China.



Replicating this coordinated use of multimodal sensory input in robotic systems remains a significant challenge, particularly for tasks that require high precision and rapid responsiveness to changing contact dynamics.

Recent progress in vision-based tactile sensors has significantly improved robotic performance in contact-rich manipulation by delivering high-resolution feedback on physical interactions, such as object deformation and force distribution [4]–[6]. Despite these advances, their broad deployment remains limited due to several practical constraints, including high manufacturing cost, bulky form factors, and poor compatibility with diverse robotic platforms. Moreover, many existing tactile sensing systems exhibit a narrow field of view and insufficient spatial resolution, which hampers their effectiveness in real-world tasks demanding both dexterity and fine-grained precision [7]–[9].

In agricultural applications such as fruit and vegetable harvesting and sorting, robots are frequently required to manipulate soft and easily damaged objects, placing high demands on tactile perception capabilities [10], [11]. However, existing visuo-tactile sensors often suffer from limited sensing areas and fragile skin materials that are prone to wear or tearing, making them unsuitable for long-term, reliable operation in harsh agricultural environments—characterized by moisture, dust, and frequent physical contact. Moreover, most current designs integrate the visuo-tactile sensor separately from the gripper actuator, resulting in complex and time-consuming replacement

procedures that fail to meet the industrial need for rapid maintenance and modular interchangeability. Compounding these issues, the high cost of existing visuo-tactile sensors significantly increases the overall system price of tactile-enabled robotic manipulators, hindering their widespread adoption in real-world industrial settings and slowing the broader deployment of intelligent manipulation systems. Consequently, there is a critical need for an integrated, low-cost visuo-tactile gripper that combines large sensing coverage, robust durability, and quick replaceability in a unified, practical design.

While vision-based imitation learning (IL) has shown strong promise in robotic manipulation tasks [12]–[14], its effectiveness in contact-rich settings remains limited by the absence of tactile feedback during training. This omission impairs a robot’s capacity to react promptly to environmental perturbations, particularly in scenarios demanding rapid sensory response and adaptive force modulation. Current tactile data collection systems have struggled to establish an effective link between visuo observations and tactile signals. Many rely either on motion capture or teleoperation setups that introduce substantial latency and require intricate calibration procedures [15], [16]. Furthermore, handheld approaches that convey tactile information through mechanical linkages often suffer from degraded signal fidelity and slower response times, further limiting their utility in real-time manipulation.

In this work, we present LVTG, a low-cost vision-based tactile gripper designed to address the aforementioned limitations and enable stable, efficient, and affordable manipulation in contact-rich environments. LVTG incorporates a visuo-tactile sensing system that delivers high-resolution tactile feedback, supporting real-time adaptation of grip force and manipulation policies. Compared to conventional tactile sensors, LVTG features a compact yet robust design with an enlarged effective sensing area, enhanced durability, modular construction, and significantly lower cost, attributes that facilitate seamless integration across diverse robotic platforms. By providing a practical and scalable approach to high-fidelity tactile perception, LVTG substantially improves robotic performance in tasks that demand precise force regulation and rapid sensory-motor response. The contributions of the paper are summarized as:

- 1) We introduce LVTG, a low-cost, vision-based tactile gripper featuring an extended sensing area and a modular mechanical design that enables rapid maintenance and cross-platform compatibility.
- 2) We employ a CLIP-inspired contrastive learning objective to align tactile embeddings with corresponding visual observations, facilitating cross-modal representation learning between vision and touch.
- 3) Comprehensive experimental validation is provided, demonstrating that manipulation policies leveraging LVTG’s multimodal sensing consistently surpass vision-only baselines in complex, contact-rich tasks.

II. RELATED WORKS

A. Tactile Sensing for Robotic Manipulation

Tactile sensing is essential for enabling robots to perform precise manipulation in contact-rich environments. Conventional approaches typically employ force/torque sensors mounted at the wrist or within robotic joints [17]–[19]. Although these sensors deliver direct measurements of interaction forces, they are often costly, susceptible to noise, and incapable of resolving fine-grained local contact information. As alternatives, various electrical tactile sensors have been investigated, including those based on capacitive [20], [21], resistive [22], [23], MEMS [24], and magnetic principles [25], [26]. While these technologies enable compact integration, they frequently face limitations such as low spatial resolution, sensitivity to environmental disturbances, and complex or non-scalable fabrication processes.

In contrast, optical tactile sensors such as GelSight, Gel-Slim, MC-Tac, and 9DTact [5], [27]–[29] utilize embedded cameras to capture high-resolution images of elastomer deformation. These systems can recover rich contact information, including surface texture, local geometry, and force distribution, rendering them highly effective for contact-rich manipulation tasks. Nevertheless, most existing vision-based tactile sensors are implemented as monolithic, custom-fabricated units that lack modularity, making rapid replacement or adaptation to different robotic end-effectors impractical. Additionally, their relatively high cost and mechanical fragility hinder broad deployment in real-world robotic applications. To address these limitations, we present LVTG, a low-cost, vision-based tactile gripper featuring an enlarged sensing area, robust construction, and a modular hardware architecture that enables quick maintenance and seamless integration across diverse platforms.

B. Dataset Collection Systems for Robot Learning

The success of robot learning, particularly imitation learning, critically relies on the availability of large-scale, high-quality demonstration datasets. To collect visuo-motor data, various teleoperation approaches have been developed, including motion capture systems enhanced with AR/VR visualization [16], [30], 3D space mice [31], [32], master-slave robotic platforms [33], [34], and wearable interfaces [15], [35]. Although these methods enable accurate recording of expert trajectories, they often involve intricate calibration procedures, incur high costs, and generally do not provide real-time tactile feedback. Alternative handheld data collection paradigms offer greater flexibility across different robot embodiments but typically employ rod-based or trigger-actuated grippers. In such designs, mechanical backlash and indirect force transmission degrade tactile signal fidelity, leading to reduced accuracy in capturing and relaying contact information. Reactive diffusion policy [16] introduces an AR-based teleoperation and slow–fast visual–tactile learning framework that explicitly incorporate high-frequency tactile feedback,

demonstrating improved robustness and generalization in contact-rich manipulation tasks.

Recent efforts, such as FreeTacMan [15], have sought to mitigate these limitations by directly coupling tactile sensing with human operators for in-situ demonstration collection. However, such systems still rely on custom-built hardware that lacks scalability and broad accessibility. In contrast, our LVTG gripper offers an open-source, modular, and easily fabricable vision-based tactile sensing solution that can be seamlessly integrated into robot learning pipelines. Its low-cost and robust mechanical design substantially reduces the barrier to acquiring high-quality visuo-tactile datasets in real-world settings.

C. Vision-Based Tactile Grippers

Several vision-based tactile grippers have been proposed to integrate tactile sensing directly into robotic manipulation systems. GelSight-based grippers [36] enable high-resolution estimation of surface contact geometry, yet their narrow field of view and mechanically fragile construction hinder robust real-world use. Similarly, MCTac and GelSlim achieve compact form factors but still demand complex calibration procedures and involve expensive fabrication processes. Recent efforts, such as 9DTact, have advanced toward more affordable and generalizable tactile sensing by supporting both 3D shape reconstruction and multi-axis force estimation. V Bo et al. [37] propose an innovative soft-rigid, tendon-driven gripper: the Double-Scoop Gripper (DSG). Its two-fingered design exploits a specialized structure to cope with constrained spaces.

Building on these advances, our LVTG achieves a practical balance among sensing resolution, mechanical robustness, and usability. By expanding the tactile sensing area and adopting a modular two-finger parallel-jaw design, LVTG delivers more stable and reliable grasping performance compared to conventional tactile sensors, while remaining low-cost and easy to replace in the event of damage. Moreover, the open-source hardware design promotes reproducibility and encourages community-driven innovation in visuo-tactile sensing for robotic manipulation.

III. LVTG DESIGN

A. Details of the Component

The proposed LVTG is designed to deliver durable, modular, and easily replaceable tactile sensing for contact-rich robotic manipulation in smart agriculture. It is a compact, integrated parallel-jaw gripper that incorporates advanced visuo-tactile sensing capabilities. As illustrated in Fig. 1, LVTG features a rectangular form factor with an integrated sloped surface, which enhances its adaptability to various object shapes. The gripper measures approximately 54.9 mm in width and 90.6 mm in length. The end-effector employs a parallel four-bar linkage mechanism to realize a two-finger parallel-jaw gripper. The linkage is actuated by a motor located at the robot wrist, which

pulls the four-bar structure to drive the symmetric opening and closing of the two fingers. This mechanical design guarantees parallel finger motion throughout the grasping process, providing stable and consistent contact geometry across different objects. This design not only ensures robust performance but also simplifies maintenance and reduces costs, making it ideal for practical applications in smart agriculture and other industries.

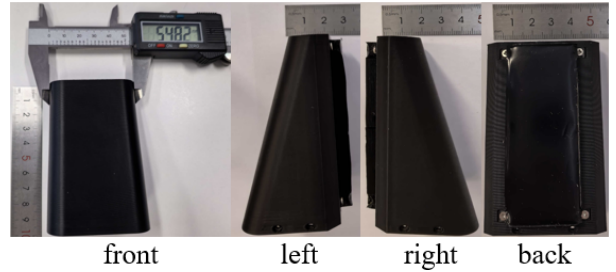


Fig. 1. The figure of LVTG's form factor.

As shown in Fig. 2(a), each visuo-tactile finger comprises a skin module, an LED illumination module, a camera module, a diffuser, a mirror, a finger shell, and a finger base. To maximize generalizability across embodied perception and data collection tasks, we adopt a parallel-jaw gripper configuration. Robustness and adaptability are further enhanced through a modular skin design and a compact optical layout that ensures uniform lighting and efficient capture of contact-induced deformations. The diffuser is designed to provide uniform illumination across the tactile surface, mitigating potential brightness imbalances from the LED array. This hardware architecture simplifies fabrication and assembly, requiring no specialized tools or expertise, while keeping the total material cost under 14.2 USD per finger.

Skin Module. The skin module follows the principle of 9DTact [5] but introduces significant modifications for durability and modularity. It consists of three layers: Black Gel Coat, Translucent Gel Layer, and Acrylic substrate (Fig. 2). Unlike 9DTact, where a transparent gel layer is prone to damage and delamination, our design directly molds the translucent silicone gel (Smooth-on Ecoflex 00-10) onto a primed acrylic plate (DOWSIL™ 1200 OS Primer), ensuring strong adhesion. The Black Gel Coat is fabricated using Smooth-on Psycho Paint with silicone pigment and Novocel Matte in a 4:4:1:2 ratio, directly cast onto the translucent gel surface. The gel thickness is optimized to ensure sensitivity to small contact deformations while maintaining durability. The chosen 3 mm thickness strikes a balance between tactile responsiveness and mechanical robustness. This modular approach allows rapid batch production of interchangeable skin modules, overcoming the fragility and irreparability issues of previous designs. As a result, LVTG significantly improves the efficiency of embodied data collection by enabling fast replacement and long-term operation.

LED Module. To achieve bright and uniform internal illumination, we design a compact LED module powered

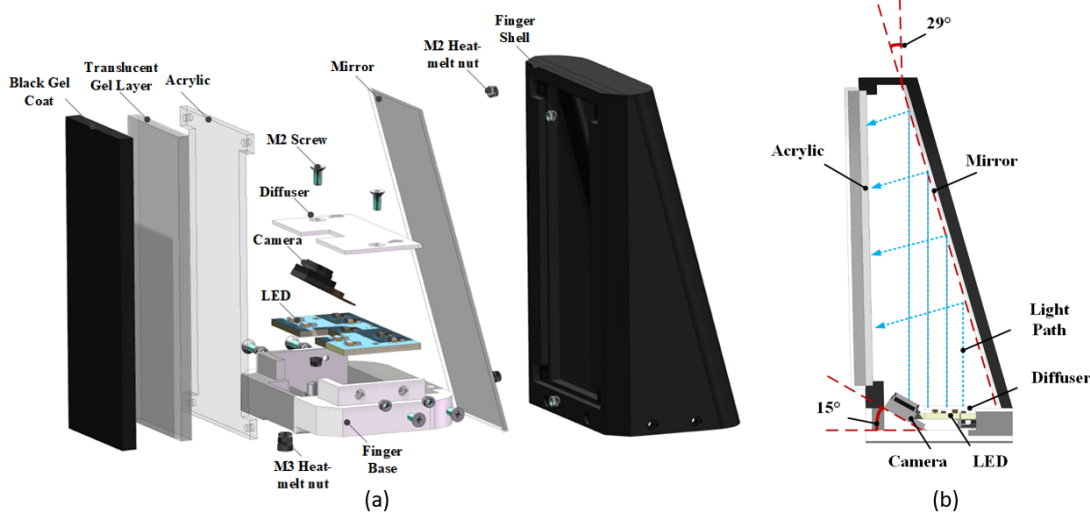


Fig. 2. (a) The exploded mechanical view of LVTG. (b) The illustration of the LVTG Optical Path.

via a standard 5V Micro-USB interface. The module incorporates nine high-intensity LEDs (TZ-P2-1206WYCS2-0.9T; luminous intensity 800–1000 mcd, color temperature 10,000–15,000 K), each individually stabilized with a $10\ \Omega$ resistor. A constant-current driver (CN5711) ensures consistent brightness across all LEDs. This design minimizes interference from external lighting and guarantees uniform illumination of the gel surface for reliable tactile imaging.

Camera Module and Optical Path. As shown in Fig. 2 (b), we employ a 3D-printed diffuser to convert the LED point sources into uniform global illumination. A mirror ($30\text{ mm} \times 65\text{ mm}$) reflects the light into the skin module while simultaneously projecting the contact deformation back toward the camera. The camera (OV5674, FoV 120°) is mounted at a 15° tilt relative to the finger base plane, enabling comprehensive capture of gel deformation and surface texture. The choice of the camera angle in the LVTG design is a critical factor for capturing accurate tactile images. The angle of 15° relative to the surface plane is chosen based on a balance between the thickness of the LVTG and the need to maximize the field of view. This angle ensures that the camera can effectively capture the contact deformations across the tactile skin while minimizing distortion at the edges. The angle also takes into account the thickness of the LVTG, ensuring that the camera remains within the optimal distance to the gel surface for clear image capture. This compact optical design achieves both high coverage and uniform lighting within a small form factor.

Finger Housing and Assembly. The finger housing consists of a Finger Shell and a Finger Base, both fabricated via 3D printing. The Finger Shell is printed in black material to absorb external light, while the Finger Base is printed in white to provide a stable mounting platform. The visuo-tactile finger is assembled in a compact and modular manner. First, the mirror is fixed to the inner slot of the Finger Shell to establish the optical path.

The skin module is then secured to the shell using four M2 screws with heat-melt nuts, ensuring firm attachment and easy replacement. The LED module and diffuser are mounted onto the Finger Base with M2 screws to provide stable illumination, while the camera module is aligned and adhered to the base at a 15° tilt for optimal contact imaging. Finally, the Finger Shell and Finger Base are fastened together with four M2 screws, completing the finger assembly. This modular design ensures straightforward fabrication, reliable structural integrity, and convenient maintenance or replacement during long-term use. To ensure compatibility with robotic platforms, the Finger Base includes five mounting holes. Four M2 holes allow direct attachment to a linear stage, while an additional M3 interface connects to linkage mechanisms. For evaluation, we integrate the LVTG fingers with the Cobot-Magic embodied platform, validating its effectiveness in visuo-tactile data collection tasks.

B. Tactile information representation pipeline

To ensure that contact information can be extracted clearly and reliably from the vision-based tactile sensor, we design a processing pipeline consisting of three key stages shown in Fig. 3: fisheye camera distortion correction, Region of Interest (ROI) extraction, and contact information enhancement.

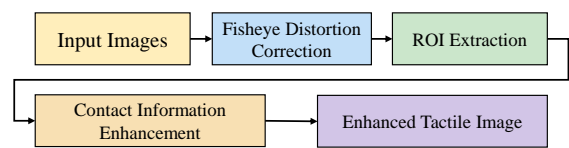


Fig. 3. The pipeline of tactile image enhancement.

Fisheye Camera Distortion Correction. The employed camera module (OV5674) has a wide field of view (120°), which introduces severe distortion, especially near the image boundaries. To prevent distortion from degrading

TABLE I
COMPARISON OF DIFFERENT VISION-BASED TACTILE SENSORS. (*MANUFACTURING OF 1000 PIECES. † COMMODITY PRICE.)

Sensor	Sensing Area [mm ²]	↑	Weight [g]	↓	FPS ↑	Cost[\$]	↓
GelSight [27]	252		NA		90	30	
GelSlim 3.0 [38]	675		45		90	25*	
DIGIT [39]	19 × 16 = 304		20		60	15* / 300†	
GelSight-Mini [29]	19 × 15 = 285		20.8		25	499†	
DTact [4]	24 × 24 = 576		78		60	34	
9DTact [5]	24 × 18 = 432		20		90	15	
LVTG (Ours)	80 × 30 = 2400		70		90	12	

the quality of the captured contact signals, we perform fisheye undistortion before deploying the camera into the sensor housing. Specifically, we capture 20 images of a 7×10 checkerboard pattern with a 15 mm square size and use OpenCV’s Fisheye Calibration procedure to estimate the intrinsic parameters and distortion coefficients. For each pixel point in the distorted image, its undistorted coordinate (x_u, y_u) is computed as,

$$\begin{bmatrix} x_u \\ y_u \end{bmatrix} = f \cdot \frac{\tan(\theta)}{r} \begin{bmatrix} x_d \\ y_d \end{bmatrix} + \begin{bmatrix} c_x \\ c_y \end{bmatrix}, \quad (1)$$

where (x_d, y_d) are distorted coordinates, f denotes focal length, (c_x, c_y) are the principal point, $r = \sqrt{x_d^2 + y_d^2}$, and $\theta = \arctan(r)$. The intrinsic matrix and distortion coefficients are estimated using 20 checkerboard calibration images. The resulting calibration model is then applied to remove distortion and obtain geometrically accurate tactile images.

ROI Extraction. Since only the gel surface contains meaningful tactile information, it is necessary to exclude irrelevant regions from the raw images. We achieve this through a three-step process: (i) a mask $M(x, y)$ of the gel surface region is generated interactively using OpenCV’s setMouseCallback function; (ii) an affine transformation is applied to rectify the irregular gel region into a rectangular patch; (iii) A pixel slicing is performed to crop the rectified gel region, which can be expressed as,

$$\begin{bmatrix} x' \\ y' \\ 1 \end{bmatrix} = A \begin{bmatrix} x \\ y \\ 1 \end{bmatrix}, \quad A \in \mathbb{R}^{2 \times 3}, \quad (2)$$

where (x, y) and (x', y') denote original and rectified coordinates, respectively. This process yields a clean ROI corresponding precisely to the tactile surface, minimizing interference from the external background.

Contact Information Enhancement. Due to the bottom-mounted LED module, vertical brightness imbalance is naturally introduced across the tactile images. To correct illumination variation and emphasize contact-induced features, we implement a contact information enhancement procedure. First, a vertical attenuation mask $W(y)$ is applied to the ROI image to normalize brightness gradients,

which can be described as,

$$I'(x, y) = I(x, y) \cdot W(y), \quad W(y) = \exp\left(-\alpha \frac{y}{H}\right), \quad (3)$$

where H is the ROI height and α controls the decay rate. Next, given the reference (no-contact) image I_{ref} and current tactile image I_{cur} , we can compute,

$$I_{\text{dark}} = \max(0, I_{\text{ref}} - I_{\text{cur}}), \quad I_{\text{bright}} = \max(0, I_{\text{cur}} - I_{\text{ref}}). \quad (4)$$

Finally, similar to the approach in 9DTact, the tactile ROI is compared with a pre-recorded reference image to compute a darker channel and a brighter channel, highlighting local deformations. The darker channel, brighter channel, and reference channel are combined into a composite enhanced tactile image, which can be described as,

$$I_{\text{enh}} = \text{Concat}(I_{\text{dark}}, I_{\text{bright}}, I_{\text{ref}}), \quad (5)$$

where $\text{Concat}(\cdot)$ denotes channel-wise concatenation, and it can serve as the final input for downstream learning algorithms.

C. Comparison of the different vision-based tactile sensors

Compared with several state-of-the-art compact vision-based tactile sensors, the proposed LVTG exhibits several distinct advantages in terms of sensing performance, mechanical robustness, and manufacturability. These key characteristics are systematically summarized and compared in the Table. I:

- **Larger Sensing Area.** The LVTG features an active sensing area of 80mm × 30mm = 2400mm², which is approximately five times greater than that of the 9DTact sensor. This expanded coverage enables the LVTG to capture more comprehensive contact information across a wider region, which is particularly beneficial for applications requiring large-area tactile perception, such as robotic grasping, object manipulation, and surface exploration. The increased spatial resolution and field of view further contribute to improved contact localization and shape estimation capabilities.
- **Enhanced Mechanical Robustness.** A critical limitation of existing designs such as the 9DTact lies in the use of a separately attached transparent gel layer,

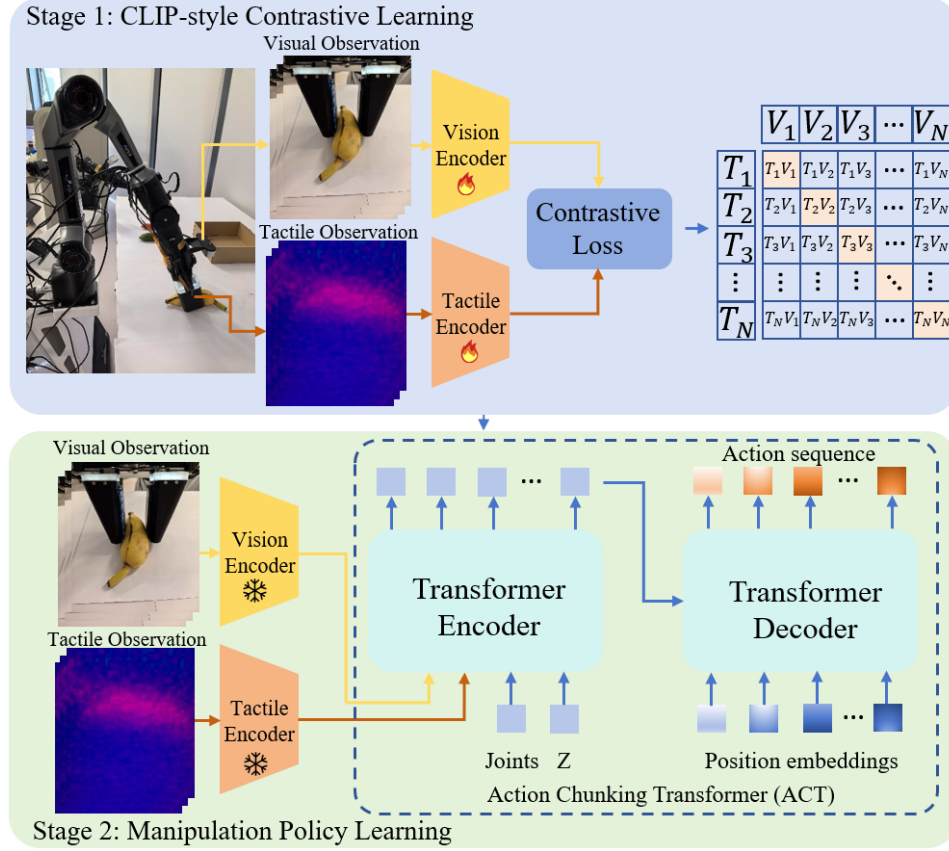


Fig. 4. The pipeline of manipulation learning.

which is prone to mechanical degradation, surface scratches, and delamination under prolonged or repetitive use. In contrast, the LVTG adopts a monolithic fabrication strategy in which a translucent silicone elastomer (Smooth-On Ecoflex 00-10) is directly cast and cured onto a chemically primed acrylic substrate (DOWSIL™ 1200 OS Primer). This co-molding process establishes strong interfacial bonding through enhanced surface adhesion, significantly reducing the risk of layer separation. Experimental evaluations under repeated indentation and sliding tests have demonstrated superior durability and long-term stability, making the sensor suitable for deployment in demanding real-world environments.

- **Low Fabrication Cost and High Manufacturability.** As detailed in the Table. I, the total material and assembly cost of the LVTG is estimated at only \$12, representing the lowest cost among all compared visuo-tactile sensing platforms. This cost efficiency is achieved through the use of inexpensive, commercially available materials and a straightforward fabrication process that does not require cleanroom facilities or complex alignment procedures. Furthermore, the modular design simplifies both initial assembly and post-deployment maintenance, allowing for rapid replacement of the sensing layer without disassembling the entire sensor unit. The combination of low cost,

ease of manufacturing, and scalability makes the LVTG a highly practical solution for large-scale deployment in robotic systems, educational platforms, and industrial automation, where affordability and reliability are critical design considerations.

D. Manipulation policy learning

We design a two-stage framework for learning visuo-tactile manipulation policies, comprising visuo-tactile contrastive learning followed by policy learning, as illustrated in Fig. 4. To enable effective tactile encoding, we collect 5000 visuo-tactile trajectories using the LVTG, forming a high-fidelity dataset for self-supervised pretraining. Although tactile signals are image-like, directly applying RGB-pretrained vision models leads to suboptimal features due to domain discrepancies in appearance and semantics [40]. To bridge this gap, we adopt a CLIP-style contrastive learning approach [41], where both the visual encoder f_v and tactile encoder f_t share a ResNet backbone initialized from the same checkpoint, with f_v kept frozen during training. Each encoder is followed by a projection head— g_v for vision and g_t for touch—with the latter concatenating tactile features with the normalized 7-DOF joint vector q_i to inject proprioceptive context. We compute normalized embeddings v_i and t_i at each timestep i , aligning t_i with v_i as the primary positive and including v_{i+1} as a secondary positive to

encourage temporal coherence, thereby capturing evolving contact patterns. The contrastive loss is computed against negatives from a fixed-size memory bank M shown in (6), where B is the batch size, τ a learning temperature, and \mathcal{N}_i indexes the negatives.

In the policy learning stage, the pretrained tactile encoder f_t is used to extract tactile representations, which are concatenated with visual embeddings and fed into an Action Chunking Transformer (ACT) [13]. The model is trained to predict sequences of absolute joint positions, enabling end-to-end visuo-tactile control for manipulation tasks. This modular design decouples representation learning from policy optimization, improving sample efficiency and generalization.

IV. EXPERIMENT

We have designed experiments to primarily verify three critical issues: Q1. Whether LVTG is more effective than other visuo-tactile sensors in terms of grasping stability and reliability, for example, when grasping a water bottle with a shifting center of gravity? Q2. The durability and service life of LVTG, as well as the convenience and speed of replacement after a malfunction occurs. Q3. Is tactile feedback improving the policy in contact-rich tasks, and how does the policy dynamically integrate visual and tactile information during the execution?

A. Grasp Stability and Reliability

We first evaluate the grasping performance of LVTG compared with a baseline gripper with 9Dtact. The experimental setup includes a set of 20 daily objects with varying shapes, sizes, weights, and surface properties (e.g., cylindrical bottles, boxes, deformable sponges, and fragile items such as eggshell containers). Each object is grasped 30 times under identical conditions, and the success rate is defined as the percentage of trials in which the object is lifted and held stably for at least 10 seconds without slipping.

As shown in Fig. 5, LVTG can stably grasp objects of different shapes and materials, such as fragile eggs and transparent wine bottles, and can clearly perceive the tactile conditions at the contact points between the gripper and the objects. This provides excellent tactile feedback for embodied manipulation. Due to its larger gripping contact area and greater opening angle, LVTG can more stably grasp unstructured objects as well as heavy and slippery objects. In particular, objects with smooth or deformable surfaces benefit from the extended tactile sensing range, enabling the gripper to adjust gripping force and contact position for more reliable manipulation.

To further evaluate the performance of LVTG relative to other visuo-tactile sensors in terms of grasp stability and generalizability, we compare the success rates of LVTG, GelSlim, and DIGIT on tasks including grasping, insertion and removal, as summarized in Table II. Due to its larger contact area and more distributed force application, LVTG achieves a higher success rate of 92%

when grasping larger and heavier objects such as wine bottles, reducing the likelihood of slippage compared to GelSlim and DIGIT. In plate-grasping tasks, LVTG's wedge-shaped design allows it to slide more easily under the plate edge, resulting in a success rate of 89%. In contrast, the cubic shapes of GelSlim and DIGIT make it more difficult to access the underside of the plate and maintain stable contact, leading to success rates of 81% and 73%, respectively. For USB insertion and removal, where the small size of the connector enables all three sensors to grasp the plug head adequately, their performance is similar, with success rates of 76%, 75%, and 73%, respectively. These results suggest that LVTG offers improved performance on certain everyday grasping tasks, particularly those involving object geometry or weight that challenge conventional sensor form factors.

TABLE II
COMPARE THE SUCCESS RATES(%) OF DIFFERENT VISION-BASED TACTILE SENSORS IN TERMS OF GRASP STABILITY AND RELIABILITY.

Vision-based Tactile Sensors	Grasping Wine Bottle	Grasping Plate	USB Insertion and Removal	Average Scores
GelSlim	85	81	76	81
DIGIT	80	73	75	76
LVTG	92	89	73	85

B. Durability and Lifespan

To validate the robustness of LVTG, we conduct a long-term durability test involving repeated grasp-release cycles. Each cycle consists of approaching the object, establishing contact, applying a grasp, and then releasing it. A total of 10,000 cycles are performed using a standard cylindrical object under controlled conditions. We monitor sensor performance degradation by tracking illumination uniformity, tactile image quality, and skin module integrity.

As illustrated in Fig. 6, LVTG demonstrates consistent sensing quality and mechanical performance throughout the experiment, with no observable gel delamination or significant signal degradation. The y-axis represents the state of health (SOH) for visuo-tactile sensors, with values ranging from 0 to 100 %, and the x-axis represents the number of operational cycles using the visuo-tactile sensors. SOH is computed as a normalized composite indicator reflecting tactile image quality and sensor functionality, including illumination uniformity, visibility of contact-induced deformation, and absence of structural damage to the sensing surface. The SOH value is normalized to the range from 0% to 100 %, with 100% corresponding to the initial sensor state. The failure threshold (80%) is chosen based on empirical observation of degraded tactile signal quality that begins to affect downstream perception performance. The curve shows that the sensor performance gradually decays with use, and it is approximately at the end of its lifespan when the performance drops below 80%. Compared to 9Dtact sensors that often fail after 1500–2000 cycles due to skin damage or optical misalignment,

$$\mathcal{L} = -\frac{1}{B} \sum_{i=1}^B \log \frac{\exp(v_i^\top t_i / \tau) + \exp(v_{i+1}^\top t_i / \tau)}{\exp(v_i^\top t_i / \tau) + \exp(v_{i+1}^\top t_i / \tau) + \sum_{j \in \mathcal{N}_i} \exp(v_j^\top t_i / \tau)} \quad (6)$$

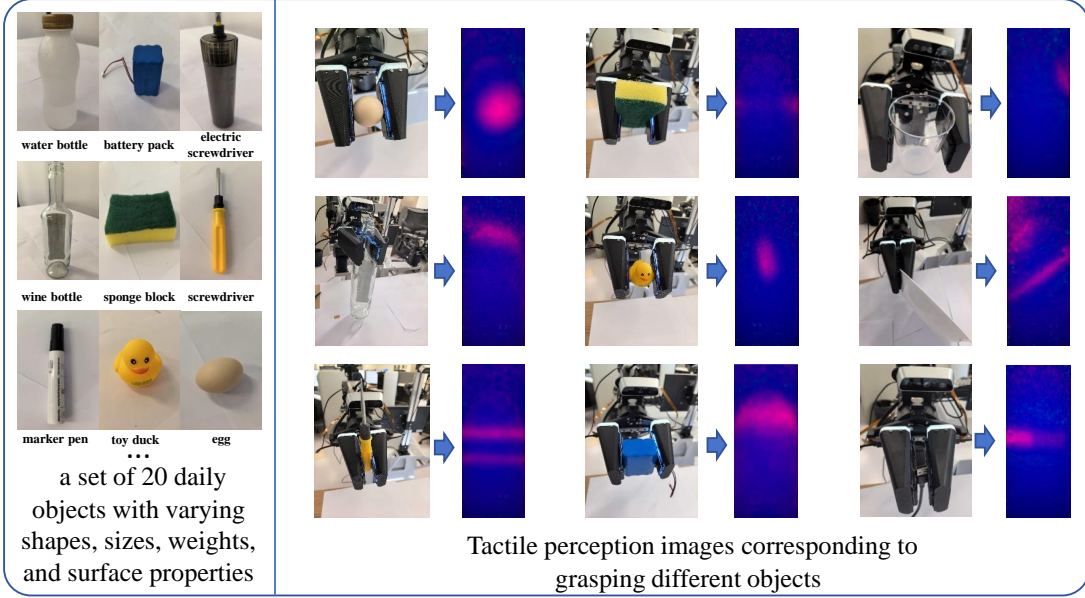


Fig. 5. Tactile perception results during grasping different objects.

LVTG exhibits over 2× longer operational lifespan. Moreover, the modular skin design allows rapid replacement when damage eventually occurs, further extending the practical service life. Notably, when the LVTG is used excessively in experiments, its performance may degrade and require replacement with a new unit. The replacement process for LVTG is very convenient: only four screws at the base connecting to the robotic arm need to be removed, and the entire procedure takes less than 30 seconds. In contrast, replacing the 9dtac requires 5 to 10 minutes and involves a more complex and cumbersome assembly process.

C. Impact of Tactile Sensing on Policy Learning

We further investigate whether the visuo-tactile feedback provided by LVTG enhances robot learning in contact-rich manipulation tasks. We adopt the ACT algorithm as the baseline imitation learning framework. Following the protocol in [40], we train two variants: (i) ACT using only visual (RGB) input; (ii) ACT augmented with both visual input and tactile images from LVTG; (iii) ACT enhanced with both visual input and tactile images by CLIP-style pretraining. Training data are collected from human demonstrations on 5 representative tasks: 1) Plate Wiping. The robot grasps a cleaning sponge and wipes the stains off the plate. 2) Fragile Cup Manipulation. The robot grasps a small plastic cup and places it on a tray without causing damage. 3) Pouring Drinks. The robot should firmly grasp the wine bottle to pour, and adapt in real time to the changing weight of the wine inside the bottle. 4) USB Plugging. The robot needs to securely insert a pre-grasped USB plug into a socket. 5) Potato Chip Grasping. The robot picks up a fragile potato chip and places it onto a plate. Each policy is trained with 200 demonstrations per task and evaluated over 50 trials.

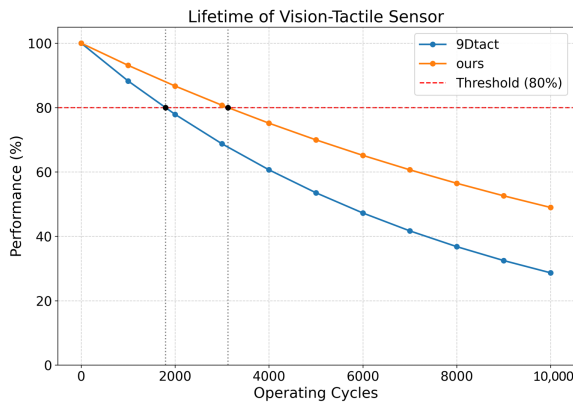


Fig. 6. The lifespan test of LVTG compared with 9Dtact.

To collect training data, we employ the COBOT Magic Robot platform [42] equipped with LVTG to teleoperate and record paired visual and tactile data across five tasks: Plate Wiping, Fragile Cup Manipulation, Pouring Drinks, USB Plugging, and Potato Chip Grasping. For each task, we gathered 1,000 teleoperated trajectories, yielding a total of 5,000 data samples. Visual and tactile image streams were published via the Robot Operating System

TABLE III
POLICY SUCCESS RATES(%) OF DIFFERENT CONTACT-RICH TASKS IN COBOT MAGIC ROBOT PLATFORM

Method	Plate Wiping	Fragile Cup Manipulation	Pouring Drinks	USB Plugging	Potato Chip Grasping	Average Scores
ACT(Vision-only)	30	35	25	25	30	29
Ours(+Tactile w/o Pretraining)	45	51	38	33	41	42
Ours(+Pretraining)	56	61	55	40	53	53

(ROS) [43] at a frequency of 30 Hz to ensure temporal synchronization between modalities. To balance storage efficiency with information retention, both visual and tactile images were captured at a resolution of 640×480 .

For negative sample construction, we avoid reliance on external datasets or complex sampling schemes and instead adopted a strategy based on standard image data augmentation. Specifically, for both tactile and visual images, we apply common augmentations including scaling (zooming in or out), random cropping, and horizontal or vertical flipping to generate view variants that are semantically inconsistent with the original samples. These variants are then used as negative samples in contrastive learning. This approach improves the model's robustness to local deformations, viewpoint changes, and noise while preserving computational efficiency. During contrastive learning, the visual tactile pair at the current time step serves as the positive sample, whereas features from augmented views of other samples and non matching pairs from different time steps collectively constitute the negative sample set. This formulation encourages the model to learn shared representations that are discriminative with respect to contact states rather than dependent on low level appearance cues. Finally, to assess the effectiveness of our pretraining strategy, we perform an ablation study comparing a baseline without tactile pretraining against a variant that incorporates contrastive learning based pretraining.

The experimental results are summarized in Table III. Without tactile feedback, the vision-only policy achieves an average success rate of only 29%. This is because the ACT algorithm cannot perceive contact information and thus struggles to regulate grip force or estimate contact area. With tactile feedback from LVTG, the success rate increases significantly to 42%. Furthermore, by aligning visual and tactile representations through CLIP-style contrastive pretraining, ACT learns implicit cross-modal correspondences that enhance skill acquisition. Compared to the non-pretrained variant, the pretrained ACT policy achieves an additional 26% improvement in task success rate. These results confirm that LVTG provides high-fidelity tactile information that complements visual perception and significantly enhances policy performance in contact-rich environments.

To validate the general applicability of the LVTG system, we conduct preliminary experiments on the Lebai LM3 robot in addition to the Cobot-Magic platform. The

LM3 is a widely used platform for industrial automation, with a six-axis articulated arm and advanced control capabilities [44]. We replicate the same set of manipulation tasks, including grasping, insertion, and removal, to evaluate the performance of LVTG on this platform. As shown in Table.IV, LVTG maintains similar performance on the Lebai LM3 platform, achieving high success rates with pretraining comparable to those observed on the Cobot-Magic platform. The modular and low-cost design of LVTG allowed for integration with the LM3, confirming that LVTG is a versatile and adaptable solution for various robotic platforms.

V. CONCLUSION

In this paper, we introduced LVTG, a low-cost visuo-tactile gripper for robust contact-rich manipulation. With a modular design and compact optics, LVTG offers a larger sensing area and wider jaw opening, enabling stable grasping of large, heavy, and fragile everyday objects. Its wear-resistant skin enhances durability, while the quick-replacement mechanism allows module swaps in under 30 seconds. Experiments show that LVTG improves grasp reliability and significantly boosts the performance of learning-based policies such as ACT when tactile feedback is used. In future work, we plan to explore online calibration methods for long-term stability and investigate bimanual collaborative manipulation to enable more complex, human-like robotic tasks involving coordinated dual-arm operations.

REFERENCES

- [1] T. Yoshioka, S. J. Bensmaia, J. C. Craig, and S. S. Hsiao, “Texture perception through direct and indirect touch: An analysis of perceptual space for tactile textures in two modes of exploration,” *Somatosensory & motor research*, vol. 24, no. 1-2, pp. 53–70, 2007.
- [2] W. M. B. Tiest and A. M. Kappers, “Cues for haptic perception of compliance,” *IEEE transactions on haptics*, vol. 2, no. 4, pp. 189–199, 2009.
- [3] D. Ma, E. Donlon, S. Dong, and A. Rodriguez, “Dense tactile force estimation using gelslim and inverse fem,” in *2019 International Conference on Robotics and Automation (ICRA)*, pp. 5418–5424, IEEE, 2019.
- [4] C. Lin, Z. Lin, S. Wang, and H. Xu, “Dtact: A vision-based tactile sensor that measures high-resolution 3d geometry directly from darkness,” *arXiv preprint arXiv:2209.13916*, 2022.
- [5] C. Lin, H. Zhang, J. Xu, L. Wu, and H. Xu, “9dtact: A compact vision-based tactile sensor for accurate 3d shape reconstruction and generalizable 6d force estimation,” *IEEE Robotics and Automation Letters*, vol. 9, no. 2, pp. 923–930, 2023.
- [6] W. Yuan, S. Dong, and E. H. Adelson, “Gelsight: High-resolution robot tactile sensors for estimating geometry and force,” *Sensors*, vol. 17, no. 12, p. 2762, 2017.

TABLE IV
POLICY SUCCESS RATES(%) OF DIFFERENT CONTACT-RICH TASKS IN LEBAI LM3 ROBOT PLATFORM

Method	Plate Wiping	Fragile Cup Manipulation	Pouring Drinks	USB Plugging	Potato Chip Grasping	Average Scores
ACT(Vision-only)	31	36	28	27	32	31
Ours(+Tactile w/o Pretraining)	46	53	41	35	42	43
Ours(+Pretraining)	58	63	56	42	55	55

[7] A. Wilson, H. Jiang, W. Lian, and W. Yuan, "Cable routing and assembly using tactile-driven motion primitives," arXiv preprint arXiv:2303.11765, 2023.

[8] S. Li, Z. Wang, C. Wu, X. Li, S. Luo, B. Fang, F. Sun, X.-P. Zhang, and W. Ding, "When vision meets touch: A contemporary review for visuotactile sensors from the signal processing perspective," *IEEE Journal of Selected Topics in Signal Processing*, vol. 18, no. 3, pp. 267–287, 2024.

[9] Z. Pan, A. Zeng, Y. Li, J. Yu, and K. Hauser, "Algorithms and systems for manipulating multiple objects," *IEEE Transactions on Robotics*, vol. 39, no. 1, pp. 2–20, 2022.

[10] J. Niu, Q. Yu, M. Bi, J. Zhao, and T. Zhang, "Deep reinforcement learning-based cooperative harvesting strategy for dual-arm robots in apple picking," *Agronomy*, vol. 15, no. 11, p. 2565, 2025.

[11] W. Mandil, V. Rajendran, K. Nazari, and A. Ghalamzan-Esfahani, "Tactile-sensing technologies: Trends, challenges and outlook in agri-food manipulation," *Sensors*, vol. 23, no. 17, p. 7362, 2023.

[12] C. Chi, Z. Xu, S. Feng, E. Cousineau, Y. Du, B. Burchfiel, R. Tedrake, and S. Song, "Diffusion policy: Visuomotor policy learning via action diffusion," *The International Journal of Robotics Research*, p. 02783649241273668, 2023.

[13] T. Z. Zhao, V. Kumar, S. Levine, and C. Finn, "Learning fine-grained bimanual manipulation with low-cost hardware," arXiv preprint arXiv:2304.13705, 2023.

[14] K. Black, N. Brown, D. Driess, A. Esmail, M. Equi, C. Finn, N. Fusai, L. Groom, K. Hausman, B. Ichter, et al., "π0: A vision-language-action flow model for general robot control. corr, abs/2410.24164, 2024. doi: 10.48550," arXiv preprint ARXIV.2410.24164.

[15] L. Wu, C. Yu, J. Ren, L. Chen, R. Huang, G. Gu, and H. Li, "Freetacman: Robot-free visuo-tactile data collection system for contact-rich manipulation," arXiv preprint arXiv:2506.01941, 2025.

[16] H. Xue, J. Ren, W. Chen, G. Zhang, Y. Fang, G. Gu, H. Xu, and C. Lu, "Reactive diffusion policy: Slow-fast visual-tactile policy learning for contact-rich manipulation," arXiv preprint arXiv:2503.02881, 2025.

[17] M. Y. Cao, S. Laws, and F. R. y Baena, "Six-axis force/torque sensors for robotics applications: A review," *IEEE Sensors Journal*, vol. 21, no. 24, pp. 27238–27251, 2021.

[18] G. G. Muscolo and P. Fiorini, "Force-torque sensors for minimally invasive surgery robotic tools: An overview," *IEEE Transactions on Medical Robotics and Bionics*, vol. 5, no. 3, pp. 458–471, 2023.

[19] S. Li and J. Xu, "Multi-axis force/torque sensor technologies: design principles and robotic force control applications: A review," *IEEE Sensors Journal*, 2024.

[20] H.-K. Kim, S. Lee, and K.-S. Yun, "Capacitive tactile sensor array for touch screen application," *Sensors and Actuators A: Physical*, vol. 165, no. 1, pp. 2–7, 2011.

[21] P. Maiolino, M. Maggiali, G. Cannata, G. Metta, and L. Natale, "A flexible and robust large scale capacitive tactile system for robots," *IEEE Sensors Journal*, vol. 13, no. 10, pp. 3910–3917, 2013.

[22] Y. Zhu, Y. Liu, Y. Sun, Y. Zhang, and G. Ding, "Recent advances in resistive sensor technology for tactile perception: A review," *IEEE sensors journal*, vol. 22, no. 16, pp. 15635–15649, 2022.

[23] Q. Shu, Y. Pang, Q. Li, Y. Gu, Z. Liu, B. Liu, J. Li, and Y. Li, "Flexible resistive tactile pressure sensors," *Journal of Materials Chemistry A*, vol. 12, no. 16, pp. 9296–9321, 2024.

[24] I. S. Bayer, "Mems-based tactile sensors: Materials, processes and applications in robotics," *Micromachines*, vol. 13, no. 12, p. 2051, 2022.

[25] J. Man, G. Chen, and J. Chen, "Recent progress of biomimetic tactile sensing technology based on magnetic sensors," *Biosensors*, vol. 12, no. 11, p. 1054, 2022.

[26] A. Alfaedhel and J. Kosel, "Magnetic nanocomposite cilia tactile sensor," *Advanced Materials*, vol. 27, no. 47, pp. 7888–7892, 2015.

[27] S. Dong, W. Yuan, and E. H. Adelson, "Improved gelsight tactile sensor for measuring geometry and slip," in *2017 IEEE/RSJ International Conference on Intelligent Robots and Systems (IROS)*, pp. 137–144, IEEE, 2017.

[28] J. Ren, J. Zou, and G. Gu, "Mc-Tac: Modular camera-based tactile sensor for robot gripper," in *The 16th International Conference on Intelligent Robotics and Applications (ICIRA2023)*, Springer, 2023.

[29] Gelsight, "Gelsight-mini." <https://www.gelsight.com/gelsightmini/>. 2022.

[30] S. Chen, C. Wang, K. Nguyen, L. Fei-Fei, and C. K. Liu, "Ar-cap: Collecting high-quality human demonstrations for robot learning with augmented reality feedback," in *2025 IEEE International Conference on Robotics and Automation (ICRA)*, pp. 8291–8298, IEEE, 2025.

[31] L. A. Bolaños, D. Xiao, N. L. Ford, J. M. LeDue, P. K. Gupta, C. Doebeli, H. Hu, H. Rhodin, and T. H. Murphy, "A three-dimensional virtual mouse generates synthetic training data for behavioral analysis," *Nature methods*, vol. 18, no. 4, pp. 378–381, 2021.

[32] R. Martin-Martin, M. Patel, H. Rezatofighi, A. Shenoi, J. Gwak, E. Frankel, A. Sadeghian, and S. Savarese, "Jrdb: A dataset and benchmark of egocentric robot visual perception of humans in built environments," *IEEE transactions on pattern analysis and machine intelligence*, vol. 45, no. 6, pp. 6748–6765, 2021.

[33] J. Aldaco, T. Armstrong, R. Baruch, J. Bingham, S. Chan, K. Draper, D. Dwibedi, C. Finn, P. Florence, S. Goodrich, et al., "Aloha 2: An enhanced low-cost hardware for bimanual teleoperation," arXiv preprint arXiv:2405.02292, 2024.

[34] Z. Fu, T. Z. Zhao, and C. Finn, "Mobile aloha: Learning bimanual mobile manipulation with low-cost whole-body teleoperation," arXiv preprint arXiv:2401.02117, 2024.

[35] C. Chi, Z. Xu, C. Pan, E. Cousineau, B. Burchfiel, S. Feng, R. Tedrake, and S. Song, "Universal manipulation interface: In-the-wild robot teaching without in-the-wild robots," arXiv preprint arXiv:2402.10329, 2024.

[36] A. C. Abad and A. Ranasinghe, "Visuotactile sensors with emphasis on gelsight sensor: A review," *IEEE Sensors Journal*, vol. 20, no. 14, pp. 7628–7638, 2020.

[37] V. Bo, L. Franco, E. Turco, M. Pozzi, M. Malvezzi, D. Pratichizzo, et al., "Design and control of soft-rigid grippers for food handling," in *ICRA2024 workshop on cooking robotics: perception and motion planning*, 2024.

[38] I. H. Taylor, S. Dong, and A. Rodriguez, "Gelslim 3.0: High-resolution measurement of shape, force and slip in a compact tactile-sensing finger," in *2022 International Conference on Robotics and Automation (ICRA)*, pp. 10781–10787, IEEE, 2022.

[39] M. Lambeta, P.-W. Chou, S. Tian, B. Yang, B. Maloon, V. R. Most, D. Stroud, R. Santos, A. Byagowi, G. Kammerer, et al., "Digit: A novel design for a low-cost compact high-resolution tactile sensor with application to in-hand manipulation," *IEEE Robotics and Automation Letters*, vol. 5, no. 3, pp. 3838–3845, 2020.

[40] A. George, S. Gano, P. Katragadda, and A. B. Farimani, "Vital

pretraining: Visuo-tactile pretraining for tactile and non-tactile manipulation policies,” in 2025 IEEE International Conference on Robotics and Automation (ICRA), pp. 258–264, IEEE, 2025.

[41] A. Radford, J. W. Kim, C. Hallacy, A. Ramesh, G. Goh, S. Agarwal, G. Sastry, A. Askell, P. Mishkin, J. Clark, et al., “Learning transferable visual models from natural language supervision,” in International conference on machine learning, pp. 8748–8763, PMLR, 2021.

[42] Y. Mu, T. Chen, S. Peng, Z. Chen, Z. Gao, Y. Zou, L. Lin, Z. Xie, and P. Luo, “Robotwin: Dual-arm robot benchmark with generative digital twins (early version),” in European Conference on Computer Vision, pp. 264–273, Springer, 2024.

[43] S. Macenski, T. Foote, B. Gerkey, C. Lalancette, and W. Woodall, “Robot operating system 2: Design, architecture, and uses in the wild,” *Science robotics*, vol. 7, no. 66, p. eabm6074, 2022.

[44] Lebai, “Lebai-lm3.” <https://www.lebai.ltd/products/lm3/>. 2022.